Non-Bloch Nature of Alloy States in a Conventional Semiconductor Alloy: $Ga_xIn_{1-x}P$ as an Example

Yong Zhang,[1,*] A. Mascarenhas,[1] and L.-W. Wang[2]

[1]*National Renewable Energy Laboratory, 1617 Cole Boulevard, Golden, Colorado 80401, USA*

[2]*Lawrence Berkeley National Laboratory, Berkeley, California 94720, USA*

(Received 10 April 2008; published 18 July 2008)

Using $Ga_xIn_{1-x}P$ as a prototype system, we present the first systematic examination of the alloy scattering effects on the global electronic structure of a semiconductor alloy for the whole composition range. Contrary to conventional wisdom, many electronic states in such a "well behaved" alloy are found to differ drastically from a Bloch state, including band edge states that are derived from degenerate critical points. This study offers a more comprehensive picture of the electronic structure of the alloy, and reveals new nontrivial but vital implications of the alloy scattering on transport and optical properties.

DOI: 10.1103/PhysRevLett.101.036403 PACS numbers: 71.23.−k, 71.20.Nr

Despite those well-known effects associated with potential fluctuations (e.g., linewidth broadening [1], reduction in carrier mobility [2]), electronic states in a conventional semiconductor alloy are generally believed to resemble Bloch states that exist only in a system with genuine translational symmetry. In other words, the deviation of an actual alloy state from that of a virtual crystal approximation (VCA) [3,4] is expected to be relatively small so that one could use a "majority representation" [5] in which an alloy state is dominated by one particular $\mathbf{k}$ vector with a spectral purity typically >0.9 (1 being the ideal value), though quantitatively the disorder results in an energy shift from the VCA value plus a spectral broadening [6,7]. However, the validity of this understanding has only been rigorously verified for alloy states near fundamental band edges and at few compositions [5]. Here we show that this perception could be *qualitatively* very inaccurate for alloy states in general, based on our analyses for the global electronic band structure of a prototype semiconductor alloy throughout the whole composition range. Specifically, it is often not true for an alloy state to have one dominant $\mathbf{k}$ component, even when it is a band edge state, unless it is derives from the nondegenerate VCA Γ point. Additionally, for the alloy band edge states derived from degenerate VCA critical points, a strong intervalley mixing due to intervalley scatterings leads to nontrivial effects on transport and optical properties, which is predicated to be important for a broad range of semiconductor alloys.

One of the best-known alloy systems, $Ga_xIn_{1-x}P$, is chosen for this study. It is generally conceived as a well-behaved alloy, and has been well studied for $x \sim 0.5$, because of the important applications for telecommunication and photovoltaics and a very interesting phenomenon—spontaneous ordering [8]. It has been indicated recently that the $Ga_xIn_{1-x}P$ alloy with x away from 0.5 holds the great promise for multijunction solar cells to reach an above 45% efficiency [9]. However, the electronic structure of this alloy is not accurately known for $x \neq 0.5$. Motivated by the general interest in the basic physics of semiconductor alloys and the practical need for this alloy system, we now perform the electronic structure calculation for the whole x range, including the major high critical points.

An improved empirical pseudopotential method is used in this study [10]. It has been shown to be able to reproduce very well not only the binary band structures but also the alloy band structure at $x \sim 0.5$, even with varying degree of ordering [11,12]. Computational details can be found in Ref. [11].

A supercell approach is used to realistically model the random alloy. For future convenience in studying the CuPt ordering that often occurs in this alloy system along the [111] direction, an orthorhombic supercell is built with three cell vectors $\mathbf{a}_1$, $\mathbf{a}_2$, and $\mathbf{a}_3$ along the $x' \sim [11\bar{2}]$, $y' \sim [\bar{1}10]$, and $z' \sim [111]$ direction of the zinc-blende (ZB) crystal, respectively [11]. The lattice constant $a(x)$ is assumed to obey Vegard's rule with $a_{GaP} = 5.447$ Å and $a_{InP} = 5.8658$ Å. A large supercell containing 27 648 atoms, with $a_1 = 12\sqrt{3/2}a$, $a_2 = 12\sqrt{2}a$, and $a_3 = 8\sqrt{3}a$, is used for most analyses, which ensures the band gap converging to within few meV [11]. Similar accuracy has been achieved for an $Al_xGa_{1-x}As$ alloy modeled by a tight-binding approach with the same order of supercell size [13]. Initially all atoms in the supercell occupy the ZB sites, but are relaxed to minimize the strain energy, using the valence force field method [14]. To solve the Schrödinger equation for the large systems involved, a folded spectrum method is used [15], which allows us to solve for only the states near the band edge within an energy range of interest. To obtain and analyze eigenstates far away from the band edge, a smaller supercell of 3456 atoms (a factor of 2 reduction in each dimension) is used. For such cases, a "representative" configuration that closely matches the average energies of band gap, conduction band minimum (CBM), and valence band minimum (VBM) from 50 different configurations is selected. The

averaged band gap of the smaller supercell is in fact very close to that of the larger one (within 1–2 meV).

Let $\varphi_i(\mathbf{r})$ be the eigenfunction of an alloy eigenstate with energy E; it can be expanded in a complete set of Bloch states $[\phi_n(\mathbf{k}, \mathbf{r})]$ with band index n and wave vector $\mathbf{k}$ defined in the Brillouin zone (BZ). A natural choice for $[\phi_n(\mathbf{k}, \mathbf{r})]$ would be the VCA solutions of the same system. The degree of how the alloy state resembles the Bloch state can be quantitatively described by a $\mathbf{k}$-space projection function [5]

$$P_i(k) = \sum_n |\langle \varphi_i(r) | \phi_n(k, r) \rangle|^2, \quad (1)$$

with $P_i(\mathbf{k}) \leq 1$. If $\varphi_i(\mathbf{r})$ is dominated by one component $\mathbf{k}_0$, we may consider this state to be primarily derived from the $\mathbf{k}_0$ Bloch state of the virtual crystal, and the spectrum of $P_i(\mathbf{k})$ reveals how many other ($\mathbf{k} \neq \mathbf{k}_0$) Bloch states the $\mathbf{k}_0$ state is coupled to by the potential fluctuation. Alternatively, one can define a spectral function [6,16]

$$A(k_0, E) = \sum_i P_i(k_0) \delta(E - E_i). \quad (2)$$

$A(\mathbf{k}_0, E)$ instead indicates to what extent the $\mathbf{k}_0$ Bloch state is mixed into other states of different energies, and is a pertinent property for a real alloy. In the supercell approach, we calculate enough eigenstates of the supercell (at $k = 0$) to include all the folded states from the Γ, L, and X point of the ZB BZ, and evaluate $P_i(k)$ for each of them. The convergence of $P_i(\mathbf{k})$ with increasing the supercell size is somewhat slower than the energy levels, especially for those high-lying states. Whenever possible, we use the results of the 27648-atom supercells for both energy and $P_i(\mathbf{k})$. However, in a few cases, because of limitations in the computational resources, we have to use the results of 3456-atom supercell, and the $P_i(\mathbf{k})$ so obtained should be considered as the upper bound.

For the whole composition range $0 \leq x \leq 1$, Fig. 1 shows the alloy energy levels derived from the three ZB critical points (Γ, L, and X) of the conduction band (CB) and from the ZB Γ point of the valence band (VB), with the corresponding $\mathbf{k}$ projection $P_i(\mathbf{k})$. The x dependences of these critical point energies are fitted with the following equation:

$$E(x) = E(0) + [E(1) - E(0)]x - b(x)x(1 - x). \quad (3)$$

We find that a bowing parameter in the form of $b(x) = b_0 + b_1 x$ can fit all the critical points very well. The fitting parameters are summarized in Table I. The results for individual critical points can be used to obtain the natural band offsets between any two compositions. The CBM Γ to X crossing occurs at $x_{\Gamma-X} = 0.749$, which agrees well with reported values: 0.74 from optical measurements [17,18], ≥ 0.73 from a mobility measurement [2], and 0.74 from a theoretical analysis [19]. Two other crossing points, L to X and Γ to L (the energy moves from lower to higher), are found to be $x_{L-X} = 0.725$ and $x_{\Gamma-L} = 0.768$, respectively, both above the CBM. The current $x_{\Gamma-X}$ value is substantially more accurate than $x_{\Gamma-X} = 0.695$ of an early calculation that also gave significantly different values for $x_{L-X} = 0.571$ and $x_{\Gamma-L} = 0.783$ [4]. Next, we should discuss the exact meanings of these results and the most profound implications of this study.

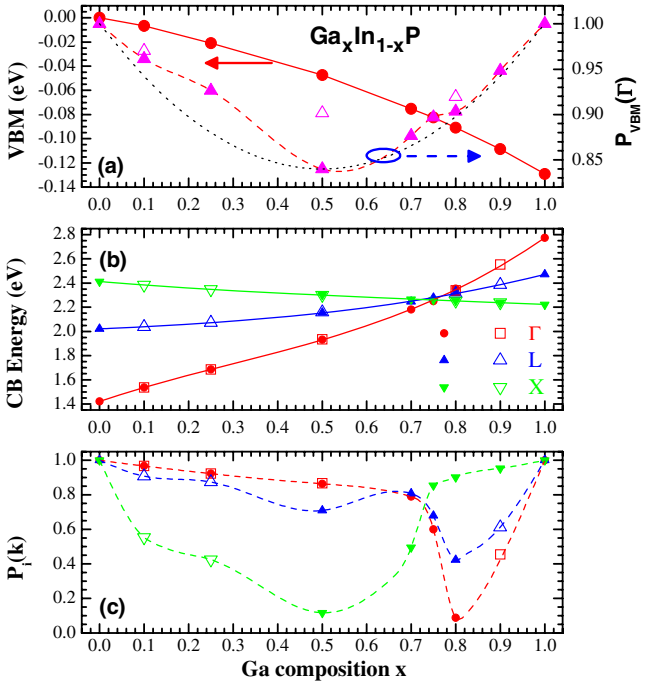

FIG. 1 (color online). Calculated critical point energies and the corresponding $\mathbf{k}$-space projections for $Ga_xIn_{1-x}P$ alloys. (a) For the valence band maximum and the $\mathbf{k}$-space projection [the dotted line for $x(1 - x)$ dependence]; (b) for the critical points of the conduction band, and (c) for the $\mathbf{k}$-space projections of the conduction band critical points. Solid symbols represent the calculated data points for 27 648-atom supercells, and open symbols for 3456-atom supercells. Solid lines are fitting curves, and dashed lines are guides to the eyes.

One of our surprising findings is that it may in fact be questionable for many alloy states to be viewed as Bloch-like states or using the majority representation, even for as little as 10% deviation from the end points $x = 0$ or 1. The degree of alloy fluctuation induced $\mathbf{k}$-space mixing sensitively depends on the number of states available for coupling or roughly the density of states, if we take the VCA Bloch states as the zero order approximation. For the VB, there are two close-by states (within 2 meV) with large and comparable Γ projections. We thus define the VBM as the weighted average of the two states by their Γ projections.

TABLE I. Fitting parameters for use with Eq. (3) (in eV).

	E(0)	$E(1)$–$E(0)$	b_0	b_1
$E_{CB}\Gamma$	1.421	1.353	0.139	1.051
E_{CBL}	2.021	0.451	0.282	0.187
E_{CBX}	2.412	−0.190	0.109	−0.079
E_{VBM}	0	−0.129	−0.056	−0.026

Figure 1(a) shows the x dependence of VBM and its Γ component $P_{\mathrm{VBM}}(\Gamma)$. Indeed, the VBM behavior is just what is expected from the conventional understanding of an alloy: the majority representation holds with $P_{\mathrm{VBM}}(\Gamma) > 0.84$, and the effect of the alloy fluctuation maximizes at $x \sim 0.5$, roughly following the $x(1-x)$ rule. The situation for the CB is nevertheless much more complex. Figure 1(b) shows x dependence for the energy levels and Fig. 1(c) for the corresponding $\mathbf{k}$ projections. For $x < 0.7$, the CBM is primarily derived from the Γ state with $P_{\mathrm{CBM}}(\Gamma)$ or $P_\Gamma > 0.80$, and thus can indeed be viewed as Bloch-like. However, the other two critical points, the L- and X-like (the definitions are given later) may contain significant contributions from other $\mathbf{k}$ points. Especially, for the X derived alloy state, the projection P_X drops to close to 0.1 at $x = 0.5$. Beyond $x = 0.7$, P_Γ dips even below 0.1 at $x \sim 0.8$, which makes it rather ambiguous to even call it Γ-like, although it does have the largest Γ component among the states within the expected energy range. The alloy fluctuation is found to induce significant splittings among the fourfold or threefold degenerate L or X point. In Fig. 1(b), the energy level of the L-like state E_L is defined as the weighted average of the 4 alloy states with the largest total L projections $P_i(L) = \sum_j^4 P_i(L_j)$, and the average L component P_L is defined by $\sum_j^4 |E_i - E_L|^{-1} P_i(L) / \sum_j^4 |E_i - E_L|^{-1}$. The X point energy E_X and the average X component P_X are defined in a similar manner. The strong variations shown in Fig. 1(c) for the $\mathbf{k}$ projections can be understood qualitatively by following the evolution of the overall CB structure with varying x. For instance, for the X-like state starting from $x = 0$, being a rather high-lying state, there are a large number of nearly degenerate VCA states that may be coupled by the potential fluctuation, therefore, the decrease of P_X with initial increase in x ($0 < x < 0.5$) is much faster than that of P_Γ when the Γ-like state is the band edge state. A similar effect has been observed in the highly mismatched alloy $GaP_{1-x}N_x$ at even lower composition ($x \sim 0.1\%$) [20]. Upon further increasing x ($0.5 < x < 0.75$), the X-like states become substantially closer to the band edge, which leads to a reduction of the states available for coupling, and concomitant with a reduction in the alloy fluctuation, P_X increases. Beyond $x > 0.75$, after the X-like state turns into the CBM, P_X becomes greater than 85%. Concurrently, the Γ-like state becomes resonant, and thus P_Γ decreases rapidly at first but recovers as x further approaching 1.

Figure 2 shows $A(k_0, E)$ for alloy states in the CB with $\mathbf{k_0} = \mathbf{k}_\Gamma$, $\mathbf{k}_L$, and $\mathbf{k}_X$ and for $x = 0.25$, 0.50, and 0.80. At $x = 0.25$ and 0.50, the high-lying X-like state shows strong mixing with nearby states; at $x = 0.80$, although only within $\sim$100 meV from the band edge, the resonant Γ-like state E_Γ, the one with the largest P_Γ, couples with many states below and above it. Although the state identified as Γ-like only has $P_\Gamma \approx 0.092$, the sum of the Γ projections for all the states below equals 0.445, and thus for all the states above should be 0.463, implied by the sum

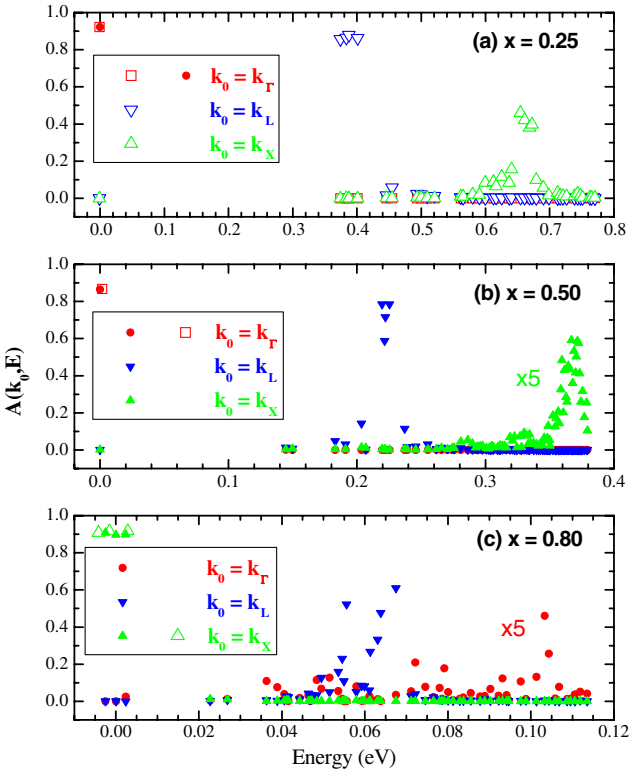

FIG. 2 (color online). Spectral function $A(k_0, E)$ of $Ga_xIn_{1-x}P$ for critical points of $\mathbf{k_0} = \mathbf{k}_\Gamma$, $\mathbf{k}_L$, and $\mathbf{k}_X$. Solid and open symbols are the results using 27 648-atom and 3456-atom supercells, respectively. Energy references are the conduction band minimums in Fig. 1(b).

rule, which explains why this state still falls on the smooth curve for the Γ-like state in Fig. 1(b). Despite the CBM being X-like at $x = 0.80$, the coupling with the Γ-like state does yield a finite Γ component $\sim$0.5%, which is sufficient to produce the zero-phonon absorption or emission at the X-like fundamental band gap [17,21]. It is worth mentioning that because of the high degeneracy of the VB, it is found that at $x = 0.50$ the spin-orbit split off band has only $\sim$45% of the Γ component, even though being merely $\sim$100 meV below the VBM, which might be reflected in the weakness of the spin-orbit feature in absorption and modulation spectra for samples with $x \sim 0.5$ [22].

Another important finding is that there is a strong intervalley mixing among the degenerate critical points $\mathbf{k_0}$'s in the VCA, even in the case where they are the CBM and have a high overall purity. Specifically, we consider the case $x = 0.80$, for which the CBM is X-like with $P_X > 0.9$, and thus at the first glance it seems to obey the majority representation [5]. However, it is found that for each individual state of all the three split X-like states, $P_i(k_X)$ has nearly equal contribution, 0.3 ± 0.2, from the three independent valleys (i.e., [100], [010], and [001]), by averaging 50 different 3456-atom configurations. This equal partition reveals the significance of the intervalley scattering in an otherwise believed simple alloy, and the large fluctuation (the standard deviation) indicates the

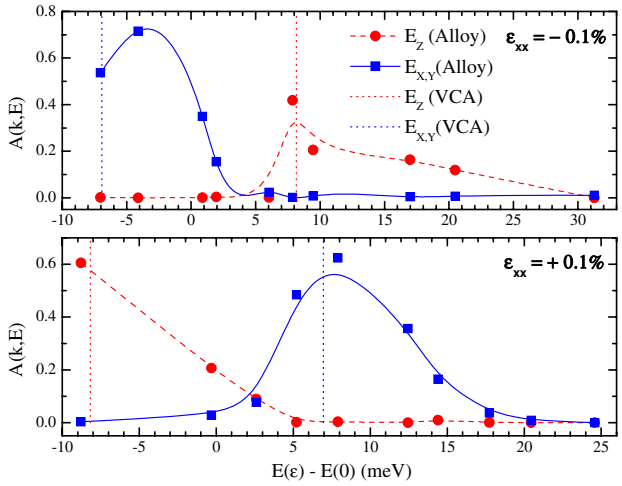

FIG. 3 (color online). The splitting of the X_1 conduction band states under (001) biaxial epitaxial strain for $Ga_{0.8}In_{0.2}P$.

sensitivity of the intervalley scattering on the detail of the atomic configuration. Similar results are obtained from a few 27 648-atom supercells. The intervalley scatterings are practically important if we further notice that the energy spread of each individual X-like state is smaller than the splittings among the three X-like states. There are, for example, two important implications: (1) on the macroscopic scale, the alloy band edge state is a uniform mixture of the three independent Bloch states associated with the three VCA $\mathbf{k}_X$ points, which is of significance for understanding certain alloy behaviors, such as the response to an uniaxial strain along an [001] type axis. For small strain, the mixture is expected to prevent the observation of the energy level splitting that would be observable in a binary. Even for moderate strain, the intervalley as well as intravalley scattering will result in a spectral broadening and quantitative deviation of the splitting from that of VCA, as shown in Fig. 3 for $Ga_{0.8}In_{0.2}P$ (using a 27 000 atom cubic supercell) under (001) biaxial epitaxial strain (Ref. [23]). (2) On the mesoscopic scale, the intervalley mixing is quite nonuniform from one domain to the other, which is of significance for instance for the electron conductivity, if an alloy is viewed as a superposition of domains of different random configurations. It is reasonable to expect that the impact to the electron mobility could be more severe in the indirect-gap than in the direct-gap composition region because of the intervalley scattering for the former, in addition to the commonly known mechanism that the indirect band gap tends to have a larger effective mass. We further note that the intervalley and intravalley scattering have comparable strength among degenerate states, which means that they should indeed be accounted for with approximately equal weights when an empirical formula is used to describe the carrier mobility in an alloy [24]. However, the strong coupling indicates that the often used perturbative treatments for the alloy scattering could be quite inadequate.

In summary, contrary to the general belief that the electronic structure of a conventional semiconductor alloy agrees qualitatively with that of the virtual crystal approximation, we have shown that only a very limited number of alloy states can indeed be appropriately viewed as Bloch-like, whereas the others may deviate drastically from Bloch states. This conclusion is expected to be generally valid for semiconductor alloys, thus, providing a more comprehensive perspective to the general understanding of the alloying effects in semiconductors.

We thank Professor W. Harrison and Dr. S. Froyen for valuable discussions. This work was supported by the DOE-OS-BES under Contracts No. DE-AC36-99GO10337 to NREL, and No. DE-AC03-76SF00098 to LBNL. The work used the computational resources of NERSC at LBNL.

*yong_zhang@nrel.gov

[1] K. K. Bajaj, Mater. Sci. Eng. **R34**, 59 (2001).
[2] H. M. Macksey *et al.*, J. Appl. Phys. **44**, 1333 (1973).
[3] L. Nordheim, Ann. Phys. (Leipzig) **9**, 607 (1931).
[4] A. B. Chen and A. Sher, *Semiconductor Alloys, Physics and Materials Engineering* (Plenum, New York, 1995).
[5] L. W. Wang *et al.*, Phys. Rev. Lett. **80**, 4725 (1998).
[6] K. C. Hass, H. Ehrenreich, and B. Velický, Phys. Rev. B **27**, 1088 (1983).
[7] R. J. Lempert, K. C. Hass, and H. Ehrenreich, Phys. Rev. B **36**, 1111 (1987).
[8] A. Mascarenhas, *Spontaneous Ordering in Semiconductor Alloys* (Kluwer Academic/PlenumPublishers, New York, 2002).
[9] R. R. King *et al.*, Appl. Phys. Lett. **90**, 183516 (2007).
[10] L.-W. Wang, J. Kim, and A. Zunger, Phys. Rev. B **59**, 5678 (1999).
[11] Y. Zhang, A. Mascarenhas, and L. W. Wang, Phys. Rev. B **63**, 201312(R) (2001).
[12] Y. Zhang, A. Mascarenhas, and L. W. Wang, Appl. Phys. Lett. **80**, 3111 (2002).
[13] F. Oyafuso *et al.*, J. Comput. Electron. **1**, 317 (2002).
[14] P. Keating, Phys. Rev. **145**, 637 (1966).
[15] L. W. Wang and A. Zunger, J. Chem. Phys. **100**, 2394 (1994).
[16] L. C. Davis, Phys. Rev. B **28**, 6961 (1983).
[17] J. Donecker and J. Kluge, Phys. Status Solidi B **71**, K1 (1975).
[18] A. Onton and R. J. Chicotka, Phys. Rev. B **4**, 1847 (1971).
[19] M. Altarell, Solid State Commun. **15**, 1607 (1974).
[20] Y. Zhang, A. Mascarenhas, and L.-W. Wang, Phys. Rev. B **74**, 041201(R)(2006).
[21] A. N. Pikhtin and A. V. Solomonov, Fiz. Tekh. Poluprovodn. **11**, 570 (1977) [Sov. Phys. Semicond. **11**, 329 (1977)].
[22] B. Fluegel *et al.*, Phys. Rev. B **55**, 13 647 (1997).
[23] Y. Zhang and A. Mascarenhas, Phys. Rev. B **57**, 12245 (1998).
[24] S. Krishnamurthy, A. Sher, and A.-B. Chen, Appl. Phys. Lett. **47**, 160 (1985); V. Venkataraman, C. W. Liu, and J. C. Sturm, Appl. Phys. Lett. **63**, 2795 (1993).